

Changes in Gut Microbiota Control Metabolic Endotoxemia-Induced Inflammation in High-Fat Diet-Induced Obesity and Diabetes in Mice

Patrice D. Cani,^{1,2} Rodrigo Bibiloni,³ Claude Knauf,² Aurélie Waget,² Audrey M. Neyrinck,¹ Nathalie M. Delzenne¹, and Rémy Burcelin²

OBJECTIVE—Diabetes and obesity are characterized by a low-grade inflammation whose molecular origin is unknown. We previously determined, first, that metabolic endotoxemia controls the inflammatory tone, body weight gain, and diabetes, and second, that high-fat feeding modulates gut microbiota and the plasma concentration of lipopolysaccharide (LPS), i.e., metabolic endotoxemia. Therefore, it remained to demonstrate whether changes in gut microbiota control the occurrence of metabolic diseases.

RESEARCH DESIGN AND METHODS—We changed gut microbiota by means of antibiotic treatment to demonstrate, first, that changes in gut microbiota could be responsible for the control of metabolic endotoxemia, the low-grade inflammation, obesity, and type 2 diabetes and, second, to provide some mechanisms responsible for such effect.

RESULTS—We found that changes of gut microbiota induced by an antibiotic treatment reduced metabolic endotoxemia and the cecal content of LPS in both high-fat-fed and *ob/ob* mice. This effect was correlated with reduced glucose intolerance, body weight gain, fat mass development, lower inflammation, oxidative stress, and macrophage infiltration marker mRNA expression in visceral adipose tissue. Importantly, high-fat feeding strongly increased intestinal permeability and reduced the expression of genes coding for proteins of the tight junctions. Furthermore, the absence of CD14 in *ob/ob CD14*^{-/-} mutant mice mimicked the metabolic and inflammatory effects of antibiotics.

CONCLUSIONS—This new finding demonstrates that changes in gut microbiota controls metabolic endotoxemia, inflammation, and associated disorders by a mechanism that could increase intestinal permeability. It would thus be useful to develop strategies for changing gut microbiota to control, intestinal permeability, metabolic endotoxemia, and associated disorders.

Diabetes 57:1470–1481, 2008

From the ¹Unit of Pharmacokinetics, Metabolism, Nutrition and Toxicology, Université catholique de Louvain, Brussels, Belgium; the ²Rangueil Institute of Molecular Medicine, Toulouse, France; and the ³Nestlé Research Center, Department of Nutrition and Health, Lausanne, Switzerland.

Corresponding author: Prof. Rémy Burcelin, Rangueil Institute of Molecular Medicine, I²MR, IFR31, Toulouse, France. E-mail: burcelin@toulouse.inserm.fr.

Received for publication 3 October 2007 and accepted in revised form 25 February 2008.

Published ahead of print at <http://diabetes.diabetesjournals.org> on 27 February 2008. DOI: 10.2337/db07-1403.

Additional information for this article can be found in an online appendix at <http://dx.doi.org/10.2337/db07-1403>.

DGGE, denaturing gradient gel electrophoresis; FITC, fluorescein isothiocyanate; IL, interleukin; LPS, lipopolysaccharide; MDA, malondialdehyde; MCP, monocyte chemoattractant protein; PAI-1, plasminogen activator inhibitor 1; RPL19, ribosomal protein L19; TBARS, thiobarbituric acid reactive substances; TNF- α , tumor necrosis factor- α ; ZO-1, zonula occludens-1.

© 2008 by the American Diabetes Association.

The costs of publication of this article were defrayed in part by the payment of page charges. This article must therefore be hereby marked "advertisement" in accordance with 18 U.S.C. Section 1734 solely to indicate this fact.

Environmental factors, such as a fat-enriched diet and a sedentary lifestyle, are the causes of the great prevalence of obesity and type 2 diabetes in the population (1). Diabetes and obesity are characterized by a low-grade inflammation whose molecular origin is unknown (2,3). However, we have recently reported that moderate increase of plasma concentration of the inflammatory reagent, the bacterial lipopolysaccharide (LPS), increased during a fat-enriched diet, and defined metabolic endotoxemia (4). We demonstrated that LPS was responsible for the onset of metabolic diseases (4), because a continuous subcutaneous low-rate infusion of LPS induced most, if not all, of the features of metabolic diseases. Most importantly, the corresponding LPS receptor CD14 knockout mouse resisted the occurrence of the diseases. LPS is a major component of the outer membrane in Gram-negative bacteria. Although the reasons for its increase in plasma during high-fat feeding were undetermined, its levels were closely correlated but not causatively demonstrated, with changes in intestinal microbiota where the Gram negative-to-Gram positive ratio increased during high-fat feeding (4). Furthermore, dietary fibers, which reduce the impact of high-fat diet on the occurrence of the metabolic diseases (5), normalized the Gram negative-to-Gram positive ratio and plasma endotoxemia (6). These data strongly suggested that intestinal microbiota could be responsible for changes of metabolic endotoxemia and for the onset of the corresponding diseases, although the causative link between intestinal bacteria, endotoxemia, and metabolic disease was not shown. Gut microbiota has recently been proposed as an environmental factor involved in the control of body weight and energy homeostasis (7–12). Germ-free mice of the same age and genetic background as conventional mice fed with a normal chow diet had a 40% lower weight (11), whereas germ-free mice colonized with the gut microbiota derived from the conventional mice increased their fat mass and developed insulin resistance within 2 weeks. In addition, germ-free mice resisted high-fat diet-induced body weight gain and fat mass development and had lower glycemia and insulinemia (9). Strikingly, these data did not provide any result with regard to the impact of the microflora on endotoxemia and inflammation. Altogether, this evidence suggests that changes in intestinal microbial composition could be responsible for increased endotoxemia in response to a high-fat diet, which in turn would trigger the development of obesity and diabetes. Therefore, we aimed at changing the intestinal microbiota by means of an antibiotic treatment to reduce the elevated concentration of plasma LPS

in high-fat diet-fed mice and in *ob/ob* mice. We further studied some mechanisms through which intestinal microbiota changes metabolic endotoxemia and the corresponding metabolic consequences.

RESEARCH DESIGN AND METHODS

Twelve-week-old male C57bl6/J mice (Charles River, Lyon, France) and 6-week-old *ob/ob* ($n = 13$) mice (C57bl6 background; The Jackson Laboratories, Bar Harbor, ME) were housed in a controlled environment (inverted 12-h daylight cycle, lights-off at 10:00 A.M.) with free access to food and water. The mice were fed a control ($n = 13$) (A04, Villemoisson sur Orge, France) or a high-fat, carbohydrate-free diet (high fat, $n = 17$) for 4 weeks. The role of the microflora was investigated by treating control (control antibiotic, $n = 13$), high-fat-fed (high-fat antibiotic, $n = 17$), or *ob/ob* (*ob/ob* antibiotic, $n = 8$) mice with antibiotics (1.0 g/l ampicillin [Sigma, St. Louis, MO] and 0.5 g/l neomycin [Sigma] in drinking water) during the experimental period. Ampicillin and neomycin are broad-spectrum antibiotics that are poorly absorbed (or unabsorbed as in the case of neomycin) and thus without any systemic effects (13). The high-fat diet contained 72% fat (corn oil and lard), 28% protein, and <1% carbohydrate, as energy content (5). To generate the *ob/ob CD14^{-/-}* mice, *CD14^{-/-}* mice (C57bl6 background) were intercrossed with *ob^{+/-}*, and F1 double heterozygotes were then used to generate the *ob/ob CD14^{-/-}* and *ob/ob* genotypes. All of the following animal experimental procedures were validated by the local ethics committee, by the Rangueil Hospital animal ethics committee, and by the Université catholique de Louvain.

RNA extraction from cecal contents. Bacterial RNAs were extracted from cecal contents using BioRobot-EZ1 (Qiagen, Hilden, Germany), according to the manufacturer's instructions. In a nutshell, cecal contents were homogenized in a bead beater for 2 min in a sterile microcentrifuge tube containing 0.3 g glass beads and 750 μ l QIAzol lysis reagent. After the addition of 150 μ l chloroform:isoamylalcohol (24:1), the samples were vortexed for 15 s and left to stand for 2–3 min at room temperature. Finally, the samples were centrifuged at 12,000g for 15 min at 4°C, and 300 μ l supernatant was loaded into the BioRobot equipment.

Denaturing gradient gel electrophoresis profiles of cecal bacteria. Bacterial RNA was amplified by RT-PCR targeting the V3 region of the 16S rRNA gene and using the universal bacterial primers HDA1-GC and HDA2 and a previously designed program (14) (HDA1-GC, 5'-CGCCCGGGGCGC GCCCGTGGCGGGCGGGGGCGGGGGGACTCCTACGGGAGGCAGCAGT; and HDA2, 5'-GTATTACCGCGCTGCTGGCAC-3'). RT-PCR was performed using a Qiagen One-Step RT-PCR kit. Electrophoresis was performed with a DCode apparatus (Bio-Rad) and 6% polyacrylamide gels with a 30–55% gradient of 7 mol/l urea and 40% (vol/vol) formamide, which increased in the direction of electrophoresis. Electrophoretic runs were in a Tris-acetate-EDTA buffer (40 mmol/l Tris, 20 mmol/l acetic acid, and 1 mmol/l EDTA) at 130 V and 60°C for 270 min. Gels were stained with SYBR Safe 1 \times (Invitrogen) for 30 min, rinsed with deionized water, and viewed by UV transillumination. Denaturing gradient gel electrophoresis (DGGE) profiles were compared by determining the Dice similarity coefficient and using the Bionumerics software package (version 4.01, Applied Maths) at a sensitivity of 1–2%.

Fecal analyses. The content of the cecum was vacuum dried. The remainder of the nondigested carbohydrates, proteins, and lipids were quantified as described previously (15,16). The total LPS content was extracted and measured as described previously (17,18).

Quantitative RT-PCR quantification of microbial cecal content. The cecal contents collected postmortem from mice were stored at –80°C. The QIAamp DNA Stool Minikit (Qiagen) was used to extract DNA from stool sample according to the manufacturer's instructions. The primers and probes used to detect *Bifidobacterium* spp. and *Lactobacillus* spp. were based on 16S rRNA gene sequences. The PCR amplification reactions were carried out as follows: 2 min at 50°C, 10 min at 95°C, followed by 45 cycles of 15 s at 95°C and 1 min at 60°C. Detection was carried out on an ABI Prism 7900 sequence detection system (Applied Biosystems, Foster City, CA). Each assay was performed in duplicate in the same run. The cycle threshold of each sample was then compared with a standard curve made by diluting genomic DNA (10-fold serial dilution) from cultures. Cell counts before DNA extraction were determined with the Neubauer hemocytometer. To determine the sensitivity and specificity of the assays, the PCR assays were confirmed using a set of intestinal bacterial species as controls. Group-specific primers based on 16S rDNA sequences PCR assay are forward *Bifidobacterium*, CGCGTCYGGTGT GAAAG; reverse *Bifidobacterium*, CCCACATCCAGCATCCA; BHQ-1-bifido, AACAGGATTAGATACCC; forward *Lactobacillus*, GAGGCAGCAGTAGG GAATCTTC; reverse *Lactobacillus*, GCAGCTTACTACTCTATCCTCTTC; BHQ-1-lacto, ATGGAGCAACGCCGC; forward *Bacteroides-Prevotella*, GAGA

GGAAGTCCCCAC; reverse *Bacteroides-Prevotella*, CGCTACTTGGCTG GTTCAG; and VIC-CCATTGACCAATATTCCTCACTGCTGCCT-TAMRA.

Glucose tolerance tests. Oral glucose tolerance tests were performed as follows: 6-h-fasted mice were injected with glucose by gavage (1 g/kg glucose, 20% glucose solution). Blood glucose was determined with a glucose meter (Roche Diagnostics, Meylan, France) on 3.5 μ l blood collected from the tip of the tail vein. In addition, to assess plasma insulin concentration, 20 μ l blood was sampled 30 min before and 15 min after the glucose challenge. The plasma was separated and frozen at –80°C.

Real-time quantitative PCR. Total RNAs from each individual adipose tissues were prepared using the TriPure reagent (Roche, Basel, Switzerland) as described previously (5). cDNA was synthesized using a reverse transcription kit (Promega, Madison, WI) from 1 μ g total RNA. PCRs were performed with an ABI Prism 7000 Sequence Detection System instrument and software (Applied Biosystems) as described previously (5). Primer sequences for the targeted mouse genes are the following: forward tumor necrosis factor- α (TNF- α), TGGGACAGTGACCTGGACTGT; reverse TNF- α , TTCGAAAGC CCATTTGAGT; forward interleukin (IL)-1, TCGCTCAGGGTCAAGAAA; reverse IL-1, CATCAGAGGCAAGGAGAAAAC; forward plasminogen activator inhibitor 1 (PAI-1), ACAGCCTTTGTCATCTCAGCC; reverse PAI-1, CCGAACCACAAAGAGAAAGGA; forward ribosomal protein L19 (RPL19), GAAGGTCAAAGGAATGTGTTC; reverse RPL19, CCTGTCTGCCTTCA CCTTGT; forward monocyte chemoattractant protein (MCP)-1, GCAGTTAAG CCCCACCTA; reverse MCP-1, CCGCCTACTCATTGGGATCA; forward F4/80, TGACAACCAGACGGCTTGTG; reverse F4/80, GCAGGCGAGGAAAAG ATAGTGT; forward NADPHox, GGTTGGGGCTGAACATTTTTC; reverse NADPHox, TCGACACACAGGAATCAGGAT; forward six-transmembrane protein of prostate 2 (STAMP2), GCATCTAGTGTCTCTGACTGGA; reverse STAMP2, TCAAATGCGGAATACCTTGCT; forward zonula occludens-1 (ZO-1), ACCCGAAACTGATGCTGTGGATAG; reverse ZO-1, AAATGGCCGGCAG AACTGTGTA; forward occludin, ATGTCGGCCGATGCTCTC; and reverse occludin, TTTGGCTGCTCTTGGGTCTGTAT. The PCR conditions were 2 min at 50°C, 10 min at 95°C followed by 40 cycles of two-step PCR denaturation at 95°C for 15 s and annealing extension at 60°C for 60 s. Each sample contained 0.5–5 ng cDNA in 1 \times SYBRGreen PCR Master Mix (Applied Biosystems) and 200 or 300 nmol/l of each primer (Eurogentec, Verviers, Belgium) in a final volume of 25 μ l. The relative amount of each studied mRNA was normalized to RPL19 rRNA levels as housekeeping gene, and the data were analyzed according to the $2^{-\Delta\Delta CT}$ method.

Adipose tissue morphometry and staining. The mean relative proportion and mean surface area of the adipocytes was estimated by a point-counting technique on paraffin-embedded tissue as described previously (4).

Intestinal permeability in vivo. This measure is based on the intestinal permeability to 4,000-Da fluorescent-dextran (Sigma-Aldrich, St. Louis, MO) as described previously (19). Briefly, 6-h-fasted mice were injected with fluorescein isothiocyanate (FITC)-dextran by gavage (600 mg/kg body wt, 125 mg/ml). After 1 h, 120 μ l blood was collected from the tip of the tail vein. The blood was centrifuged at 4°C, 12,000g, for 3 min. Plasma was diluted in an equal volume of PBS (pH 7.4) and analyzed for FITC-dextran concentration with a fluorescence spectrophotometer (HTS-7000 Plus-plate-reader; Perkin Elmer, Wellesley, MA) at the excitation wavelength of 485 nm and the emission wavelength of 535 nm. Standard curves for calculating the FITC-dextran concentration in the samples were obtained by diluting FITC-dextran in nontreated plasma diluted with PBS (1:2 [vol/vol]).

Biochemical analyses. Plasma LPS concentration was determined using a kit based on a Limulus amoebocyte extract (LAL kit endpoint-QCL1000; Cambrex BioScience, Walkersville, MD), where samples were diluted 1/40 to 1/100 and heated for 10 min at 70°C. Internal control of recovery calculation was included in the assessment. Plasma insulin concentration was determined in 5 μ l plasma using an ELISA kit (Mercodia, Uppsala, Sweden) and following the manufacturer's instructions. Visceral adipose tissue oxidative stress level was evaluated by measuring lipid peroxidation and reactive compounds such as malondialdehyde (MDA) and 4-hydroxynonenal, natural byproducts of lipid peroxidation. The aldehydic secondary products of lipid peroxidation are accepted markers of oxidative stress. Thiobarbituric acid reactive substances (TBARS) constitute a well-established assay for screening and monitoring lipid peroxidation. The adducts formed in samples, due to the reaction between MDA with thiobarbituric acid, were measured spectrophotometrically. TBARS levels were determined from a MDA equivalence standard.

Statistical analysis. Results are presented as means \pm SE. The statistical significance of differences was analyzed by one-way ANOVA followed by post hoc (Bonferroni's multiple comparison test) or Pearson's correlation using GraphPad Prism version 4.00 for Windows (GraphPad Software, San Diego, CA; www.graphpad.com). Data with different superscript letters are significantly different ($P < 0.05$) according to the post hoc ANOVA statistical analysis.

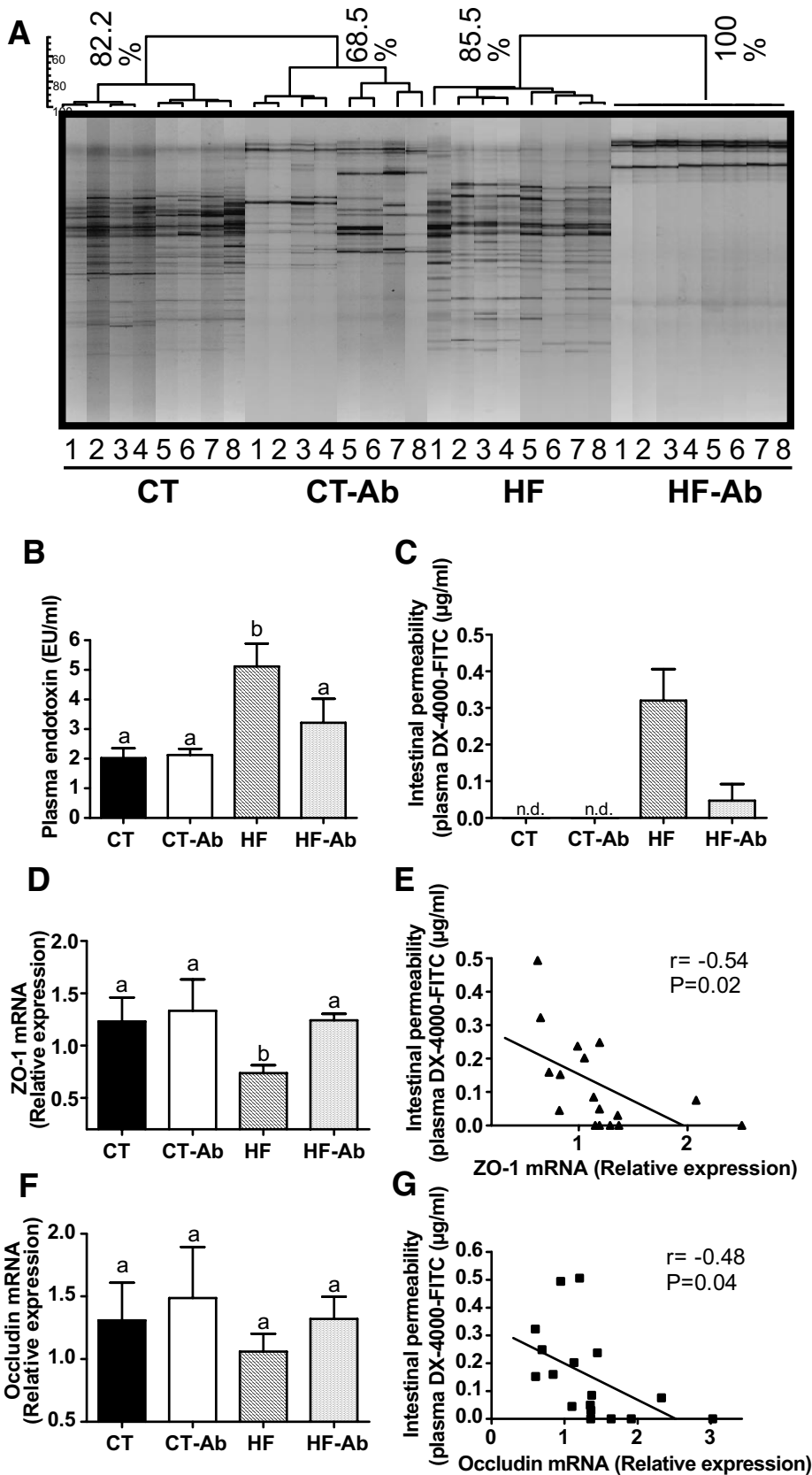


FIG. 1. Antibiotic treatment-associated changes in gut microbiota, intestinal permeability, and endotoxemia during high-fat feeding. **A:** DGGE profiles generated from the cecal microbiota in mice fed normal diet (CT), normal diet and antibiotics (CT-Ab), high-fat diet (HF), or high-fat diet and antibiotics (HF-Ab) for 4 weeks. Each number and profile corresponds to a different animal. Bar = Dice's similarity coefficient. **B:** Plasma endotoxin (LPS) concentration (EU/ml). Data are means \pm SE. Data with different superscript letters are significantly different ($P < 0.05$), according to the post hoc ANOVA statistical analysis. **C:** Intestinal permeability assay: Plasma DX-4000-FITC ($\mu\text{g/ml}$). n.d., not detectable concentration. **D** and **F:** Epithelial tight junction proteins markers (ZO-1 and occludin mRNA concentrations). **E** and **G:** Correlations between intestinal permeability markers: plasma DX-4000-FITC and epithelial tight junction ZO-1 and occludin mRNA concentrations ($P < 0.05$). *Inset* corresponds to Pearson's r correlation and corresponding P value. Data are means \pm SE. Data with different superscript letters are significantly different ($P < 0.05$) according to the post hoc ANOVA statistical analysis.

RESULTS

Antibiotic treatment-associated changes in gut microbiota and endotoxemia during high-fat feeding. We previously showed that high-fat feeding changed gut microbiota and increased plasma LPS levels, as defined

by metabolic endotoxemia (4). This was confirmed as assessed by the DGGE analysis (Fig. 1A). Therefore, to establish a cause and effect relationship according to which changes in gut microbiota initiated metabolic endotoxemia, we used large-spectrum antibiotics to

TABLE 1
Bacterial quantification

	<i>Lactobacillus</i> spp. (cells/g cecal content)	<i>Bifidobacterium</i> spp. (cells/g cecal content)	<i>Bacteroides-Prevotella</i> spp. (cells/g cecal content)
Control	6.610 ⁸ ± 3.410 ⁸ a	4.810 ⁶ ± 1.110 ⁶ a	4.710 ⁸ ± 5.810 ⁸ a
High fat	3.010 ⁷ ± 5.710 ⁶ b	5.910 ⁵ ± 2.210 ⁵ a	1.210 ⁹ ± 6.410 ⁸ b
Control antibiotic	2.110 ⁵ ± 3.810 ⁴ c	1.010 ⁴ ± 4.910 ³ b	5.110 ⁷ ± 4.410 ⁷ c
High-fat antibiotic	3.910 ⁵ ± 5.310 ⁴ c	4.510 ⁴ ± 2.310 ⁴ b	2.110 ⁸ ± 1.910 ⁸ a
<i>ob/ob</i> control	3.810 ⁹ ± 1.210 ⁹ a	8.510 ⁶ ± 3.810 ⁶ a	1.510 ⁸ ± 7.6 10 ⁷
<i>ob/ob</i> antibiotic	1.810 ⁶ ± 5.710 ⁵ b	1.410 ⁶ ± 4.110 ⁵ b	Nondetectable

Data are means ± SE. Data with different letters are significantly different ($P < 0.05$) according to the post hoc ANOVA or Student's t test statistical analysis.

modify the intestinal microbial community in mice and assessed the main features of high-fat diet-induced metabolic disorders. A 4-week antibiotic treatment strongly changed gut microbiota mRNA and bacterial content profile in both control and high-fat-treated mice (Fig. 1A; Table 1). DGGE profiles clearly showed that cecal bacterial composition and/or metabolic activity were strongly affected after a 4-week antibiotic treatment regardless of the diet (Fig. 1A). Similarity analysis

of DGGE profiles of cecal bacterial communities showed that the profiles of chow-fed animals and those of chow-fed animals treated with antibiotics were only 44% similar. This difference was even more dramatic between the high-fat-fed and high-fat-fed, antibiotic-treated mice (high-fat antibiotic), where the profiles were only 22% similar. After antibiotic treatment, each individual animal showed identical bacterial profiles (Dice's coefficient 100%). Moreover, we showed that

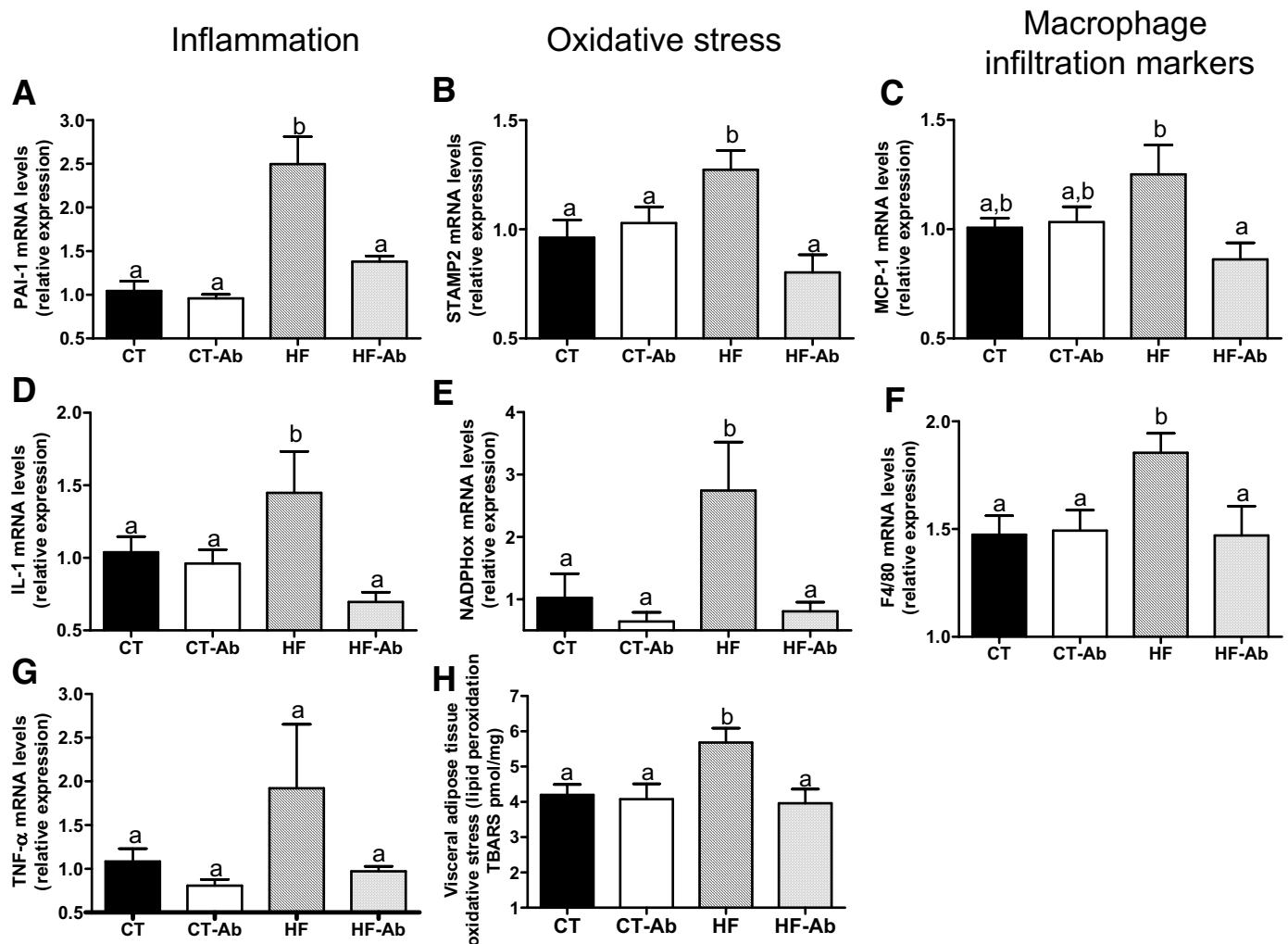


FIG. 2. Antibiotic treatment reduced the occurrence of visceral adipose tissue inflammation, oxidative stress, and macrophage infiltration markers in high-fat diet-fed mice. Inflammation: PAI-1, IL-1, and TNF- α mRNA concentrations (A, D, and G); oxidative stress: STAMP-2 and NADPHox mRNA concentrations (B and E); macrophage infiltration markers: MCP-1 and F4/80 mRNA concentrations (C and F), visceral adipose tissue oxidative stress levels (lipid peroxides concentrations) (H) in mice fed normal diet (CT), normal diet and antibiotics (CT-Ab), high-fat diet (HF), or high-fat diet and antibiotics (HF-Ab) for 4 weeks. Data are means ± SE. Data with different superscript letters are significantly different ($P < 0.05$) according to the post hoc ANOVA statistical analysis.

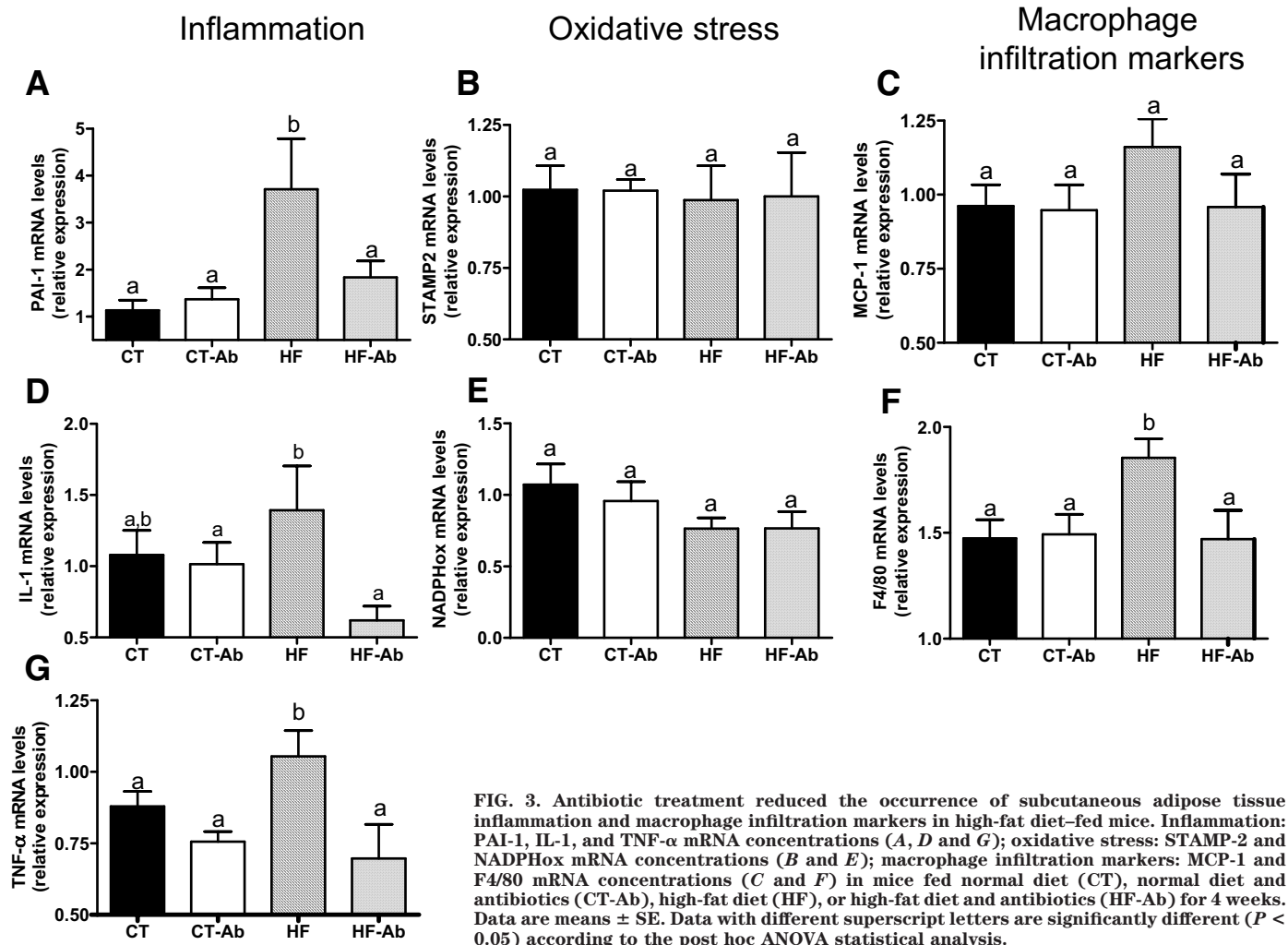


FIG. 3. Antibiotic treatment reduced the occurrence of subcutaneous adipose tissue inflammation and macrophage infiltration markers in high-fat diet-fed mice. Inflammation: PAI-1, IL-1, and TNF- α mRNA concentrations (A, D and G); oxidative stress: STAMP-2 and NADPHox mRNA concentrations (B and E); macrophage infiltration markers: MCP-1 and F4/80 mRNA concentrations (C and F) in mice fed normal diet (CT), normal diet and antibiotics (CT-Ab), high-fat diet (HF), or high-fat diet and antibiotics (HF-Ab) for 4 weeks. Data are means \pm SE. Data with different superscript letters are significantly different ($P < 0.05$) according to the post hoc ANOVA statistical analysis.

high-fat diet dramatically changed the gut microbiota content. This was characterized by a strong reduction of some Gram-positive and -negative bacteria (*Lactobacillus* spp., *Bifidobacterium* spp., and *Bacteroides-Prevotella* spp.) (Table 1). The reduced cecal microbiota content of high-fat antibiotic-treated mice only was associated with reduced metabolic endotoxemia to be similar to that of the control mice (Fig. 1B). Similarly, the cecal endotoxin content per gram of cecal content was significantly decreased after antibiotic treatment (cecal endotoxin content: control, $2.00^a \pm 0.04$ log $\mu\text{g/g}$; control antibiotic, $1.30^b \pm 0.26$ log $\mu\text{g/g}$; high fat, $0.93^c \pm 0.07$ log $\mu\text{g/g}$; high-fat antibiotic, $0.02^d \pm 0.2$ log $\mu\text{g/g}$). Moreover, we found that high-fat diet-induced metabolic endotoxemia depended on a mechanism involved in the control of gut permeability. We demonstrated that high-fat feeding dramatically increased intestinal permeability (Fig. 1C) by a mechanism associated with a reduced expression of epithelial tight junction proteins such as ZO-1 and Occludin (Fig. 1D–G), although only a tendency was observed for occludin. This effect was completely restored by the antibiotic treatment. These data suggest that gut bacteria are involved in the control intestinal permeability and furthermore in the occurrence of metabolic endotoxemia.

Antibiotic treatment reduced the occurrence of adipose tissue inflammation, oxidative stress, and macrophage infiltration markers in high-fat diet-fed mice. To causally link changes of gut microbiota to high-fat

diet-induced markers of metabolic disorders, we quantified the mRNA concentrations of PAI-1, IL-1, and TNF- α in visceral (mesenteric) adipose tissue. All mRNA concentrations were increased in high-fat diet-fed mice when compared with control-fed mice. This increase was totally blunted in the high-fat diet-fed, antibiotic-treated mice (Fig. 2A, D, and G). Inflammation and metabolic disorders are frequently associated with oxidative stress in adipose depots (20–22). We found that high-fat feeding increased STAMP2 (21) and NADPHox mRNA concentrations and lipid peroxidation, which were totally normalized by the antibiotic treatment (Fig. 2B, E, and H). Similarly, the mRNA concentrations of chemokine MCP-1 and a marker specific of mature macrophages, F4/80, were increased in high-fat mice and totally normalized by the antibiotic treatment (Fig. 2C and F). The microflora therefore appears to be a key link between high-fat feeding, plasma LPS, and visceral adipose tissue inflammation. As reported for the visceral adipose depots, the mRNA concentrations of PAI-1, IL-1, TNF- α , and F4/80 were increased in the subcutaneous adipose depots of high-fat diet-fed mice as well (Fig. 3A, D, G, and F), whereas this increase was totally blunted in the high-fat diet-fed, antibiotic-treated mice. However, no significant change was observed for STAMP2, NADPHox, and MCP-1 mRNA (Fig. 3B, C, and E). **Metabolic endotoxemia positively correlated with inflammation, oxidative stress, and macrophage infil-**

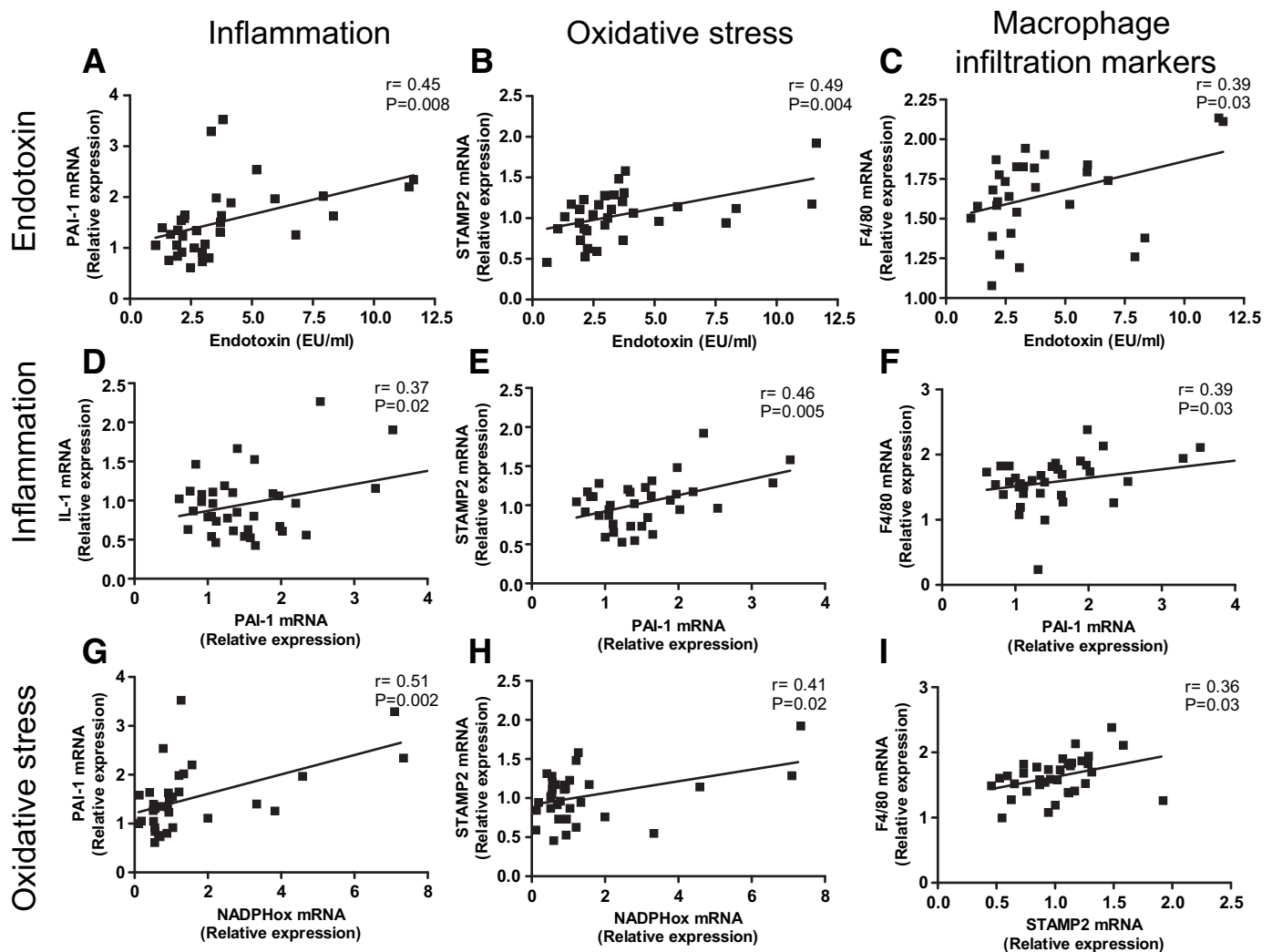


FIG. 4. Metabolic endotoxemia positively correlated with inflammation, oxidative stress, and macrophage infiltration markers. Correlations between plasma endotoxin (LPS, EU/ml) and PAI-1 (A), STAMP2 (B), and F4/80 (C) mRNA concentrations; correlations between PAI-1 mRNA concentrations and IL-1 (D), STAMP2 (E), and F4/80 mRNA (F) concentrations; correlations between NADPHox mRNA concentrations and PAI-1 (G), STAMP2 (H), and F4/80 mRNA (I) concentrations in the visceral adipose depots of mice fed normal diet (CT), normal diet and antibiotic (CT-Ab), high-fat diet (HF), or high-fat diet and antibiotics (HF-Ab) for 4 weeks. $P < 0.05$, inset corresponds to Pearson's r correlation and corresponding P value.

tration markers. To identify whether the changes of gut microbiota and metabolic endotoxemia controlled visceral adipose tissue inflammation, oxidative stress, and macrophage infiltration, we performed multiple correlation analyses between these parameters. Metabolic endotoxemia positively and significantly correlated with PAI-1, IL-1, TNF- α , STAMP2, NADPHox, MCP-1, and F4/80 mRNA (Fig. 4A–C; Supplemental Fig. 1, which is detailed in the online appendix [available at <http://dx.doi.org/10.2337/db07-1403>]). With the same aim in view, we performed other correlations and found that all inflammatory markers, oxidative stress, and macrophage infiltration markers positively and significantly correlated with one another (Fig. 4D–I). Altogether, these multiple correlations support a strong relationship between gut microbiota, endotoxemia, inflammation, and oxidative stress during high-fat diet feeding.

Antibiotic treatment prevented high-fat diet-induced adipocyte hypertrophy. We previously reported that a high-fat diet increased the adipocyte cell size (4), and here, we confirmed these data (Fig. 5A, B, and D). Furthermore, we also assumed that it could be due to a LPS-dependent

mechanism (4). Therefore, we wondered whether reduced metabolic endotoxemia, induced by the antibiotic treatment, was associated with changes in adipocyte cell size. The mean adipocyte size was reduced in high-fat antibiotic-treated mice when compared with high-fat untreated mice (Fig. 5A, B, and D). These changes were accompanied with a lower cell density when compared with all of the groups (Fig. 5C).

Antibiotic treatment improved metabolic parameters of diabetes and obesity in high-fat diet-fed mice. High-fat feeding induced glucose intolerance because the blood glucose concentrations were all higher than those of the control mice during the glucose challenge (Fig. 6A). High-fat mice treated with antibiotics exhibited improved glucose tolerance when compared with untreated mice (Fig. 6A). However, the blood glucose profiles and the calculated area under curve were still significantly different from the control-fed mice. Furthermore, glucose-induced insulin secretion, insulin resistance index, body weight gain, total energy intake, and visceral and subcutaneous adipose weight were significantly higher in high-fat diet-fed mice when compared with all of the other

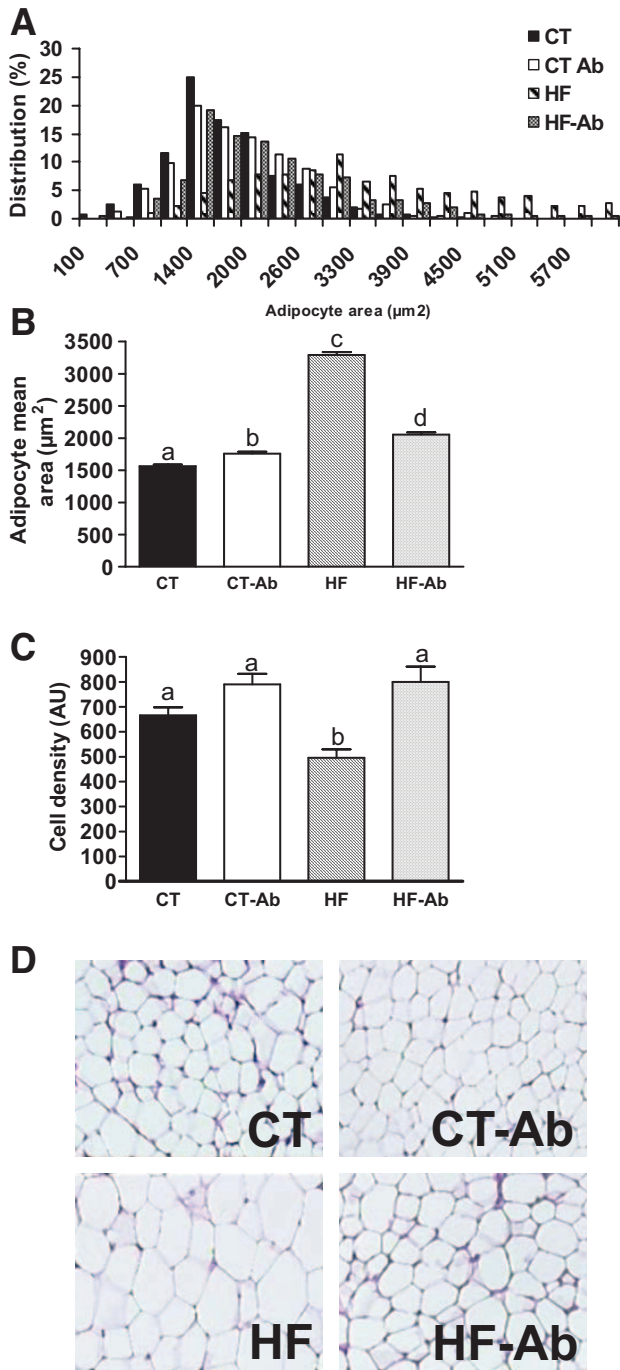


FIG. 5. Antibiotic treatment prevented high-fat diet-induced adipocyte hypertrophy. **A:** Adipocyte size distribution (%). **B:** Adipocyte mean area (μm^2). **C:** Cell density (arbitrary unit). **D:** Representative adipose tissue staining in mice fed normal diet (CT), normal diet and antibiotics (CT-Ab), high-fat diet (HF), or high-fat diet and antibiotics (HF-Ab) for 4 weeks. Data are means \pm SE. Data with different superscript letters are significantly different ($P < 0.05$) according to the post hoc ANOVA statistical analysis.

groups (Fig. 6B–H). All of the parameters were corrected by the antibiotic treatment, except for the energy intake after high-fat diet feeding, which was worsened during antibiotic treatment (Fig. 6F). This increased energy intake could be related to an impaired energy harvesting. Fecal energy content per gram cecum content was similar between groups. It was $3.16^a \pm 0.5$, $3.28^a \pm 0.04$, $3.11^a \pm 0.05$, and $3.23^a \pm 0.08$ kcal/g, in control, control antibiotic,

high fat, and high-fat antibiotic, respectively. However, the total cecal content was decreased after high-fat feeding (control $0.45^a \pm 0.02$ vs. high fat $0.19^c \pm 0.01$ g) and significantly increased after antibiotic treatment (control antibiotic $1.36^b \pm 0.08$ and high-fat antibiotic $0.82^d \pm 0.03$ g). Consequently, the total cecal energy content was increased fourfold in high-fat antibiotic ($2.85^d \pm 0.05$ kcal) when compared with high-fat mice ($0.68^c \pm 0.08$ kcal). A similar trend was observed in control ($1.42^a \pm 0.38$ kcal) versus control antibiotic ($4.63^b \pm 0.31$ kcal). The total cecal lipid content was sixfold increased in high-fat antibiotic ($34.38^c \pm 5.52$ mg) when compared with high-fat mice ($5.54^a \pm 0.44$ mg). This increase was more moderate in control ($8.81^a \pm 0.11$ mg) versus control antibiotic ($18.36^b \pm 1.84$ mg).

Antibiotic treatment of *ob/ob* mice reduced endotoxemia. To assess the contribution of gut microbiota to the development of metabolic endotoxemia and inflammation regardless of the high-fat feeding, we turned to *ob/ob* mice. These animals are characterized by higher inflammatory tone and plasma LPS concentration, whereas they are consuming a normal chow (23). Almost no bacterial RNAs were detected in any of the cecal contents of *ob/ob* mice treated with antibiotics, thus suggesting that similar to high-fat mice, the antibiotic treatment had a dramatic effect on the *ob/ob* intestinal microbial population. This could be due to the increased food intake and therefore antibiotic intake as well. Bacterial quantification confirms the DGGE profile and shows significant decrease in *Lactobacillus* spp., *Bifidobacterium* spp., and *Bacteroides-Prevotella* spp. (Table 1). Furthermore, our data showed that the treatment of *ob/ob* mice reduced metabolic endotoxemia (Fig. 7A and B). However, endotoxemia still remained higher than control values.

Antibiotic treatment of *ob/ob* mice lowered the mRNA concentration of adipose tissue inflammatory markers and metabolic parameters of diabetes and obesity. The mRNA concentrations of PAI-1 and F4/80 were significantly reduced in the visceral adipose depots and to a lower extent in the subcutaneous adipose depots of *ob/ob* antibiotic-treated mice (Fig. 7H, I, L, and M). Similarly, visceral adipose depot lipid peroxides, markers of oxidative stress, were twofold lower in antibiotic-treated mice (Fig. 7N). Moreover, glucose intolerance (Fig. 7C), insulin resistance index (Fig. 7F), glucose-induced insulin secretion (Fig. 7E), and visceral and subcutaneous adipose tissue weights (Fig. 7J and K) were reduced by the antibiotic treatment. However, no significant change of body weight was detected (Fig. 7G).

The lack of the LPS receptor CD14 partially reverted inflammatory markers and metabolic parameters in *ob/ob* mice. We and others previously demonstrated that the lack of LPS receptor protects against the high-fat diet-induced adipose tissue inflammation and metabolic disorders (4,24–28). To demonstrate that the LPS receptor might be involved in the inflammatory phenotype of *ob/ob* mice, we generated *ob/ob CD14^{-/-}* mice. We showed here that in *ob/ob CD14^{-/-}* mice, PAI-1 and F4/80 mRNA concentrations were reduced in the visceral adipose depots (Fig. 7H and L). This was accompanied by a reduction of oxidative stress markers (Fig. 7N). All of these parameters remained unchanged in the subcutaneous adipose depot when compared with *ob/ob* mice showing that CD14-mediated inflammation targeted visceral fat. Furthermore, blood glucose profiles, insulin resistance index, glucose-induced insulin secretion, visceral and subcutane-

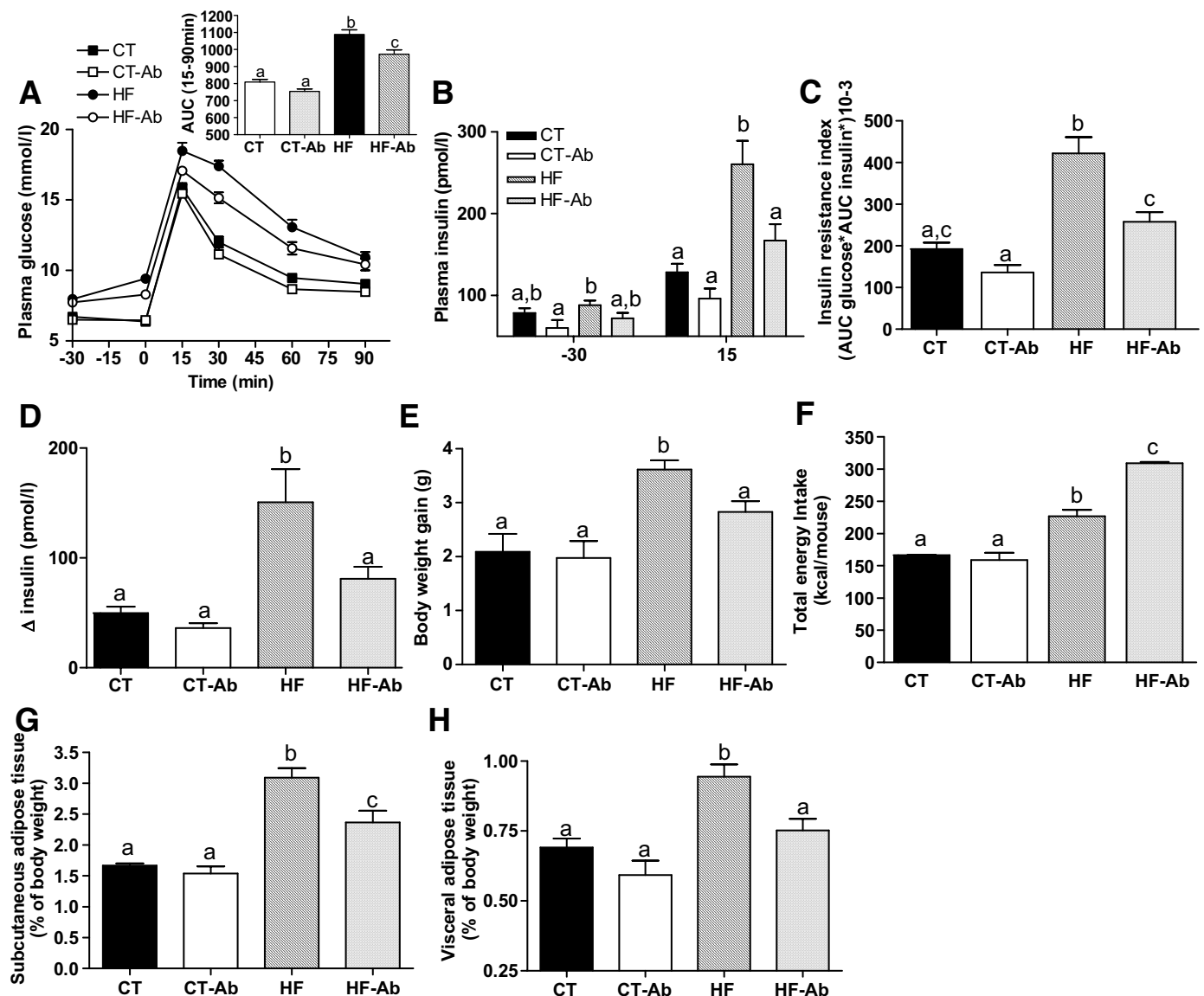


FIG. 6. Antibiotic treatment improved metabolic parameters of diabetes and obesity in high-fat diet-fed mice. **A:** Plasma glucose (mmol/l) after an oral glucose load (1 g/kg) in mice fed normal diet (CT), normal diet and antibiotics (CT-Ab), high-fat diet (HF), or high-fat diet and antibiotics (HF-Ab) for 4 weeks. The inset represents the area under curve (AUC) of the same groups. **B:** Plasma insulin concentration (pmol/l) 30 min before (-30) and 15 min after (15) oral glucose administration of the same groups. **C:** Insulin resistance index. **D:** Glucose-induced insulin secretion after oral glucose administration. **E:** Body weight gain. **F:** Total energy intake. **G:** Subcutaneous adipose tissue weight (percent body weight). **H:** Visceral adipose tissue weight (percent body weight) in mice fed normal diet (CT), normal diet and antibiotics (CT-Ab), high-fat diet (HF), or high-fat diet and antibiotics (HF-Ab) for 4 weeks. Data are means \pm SE. Data with different superscript letters are significantly different ($P < 0.05$) according to the post hoc ANOVA statistical analysis.

ous adipose tissue weights, and lipid peroxidation were reduced in *ob/ob CD14^{-/-}* when compared with *ob/ob* mice (Fig. 7C-N).

DISCUSSION

We reported here that gut bacteria are involved in high-fat diet and *ob/ob*-induced metabolic endotoxemia, adipose tissue inflammation, and metabolic disorders. This effect could be mediated by a mechanism that could increase gut permeability and enhance LPS absorption. Antibiotic treatment significantly lowers plasma LPS levels, gut permeability, and the occurrence of visceral adipose tissue inflammation, oxidative stress, macrophage infiltration, and metabolic disorders. We therefore conclude that gut

microbiota could control intestinal permeability, which determines the threshold at which metabolic endotoxemia-induced metabolic disorders occur.

We and others have recently demonstrated that the mechanisms of high-fat diet-induced inflammation and metabolic disorders were clearly linked to LPS (4,24-28). We here confirm these data and further demonstrate that this mechanism was linked to endotoxemia. We identified here that metabolic endotoxemia was due to changes in intestinal microbiota, because the antibiotic treatment, which dramatically reduced the local intestinal microbiota, restored normal plasma LPS values in high-fat diet-fed mice. High plasma LPS levels could result from an increased production of endotoxin by a change in gut

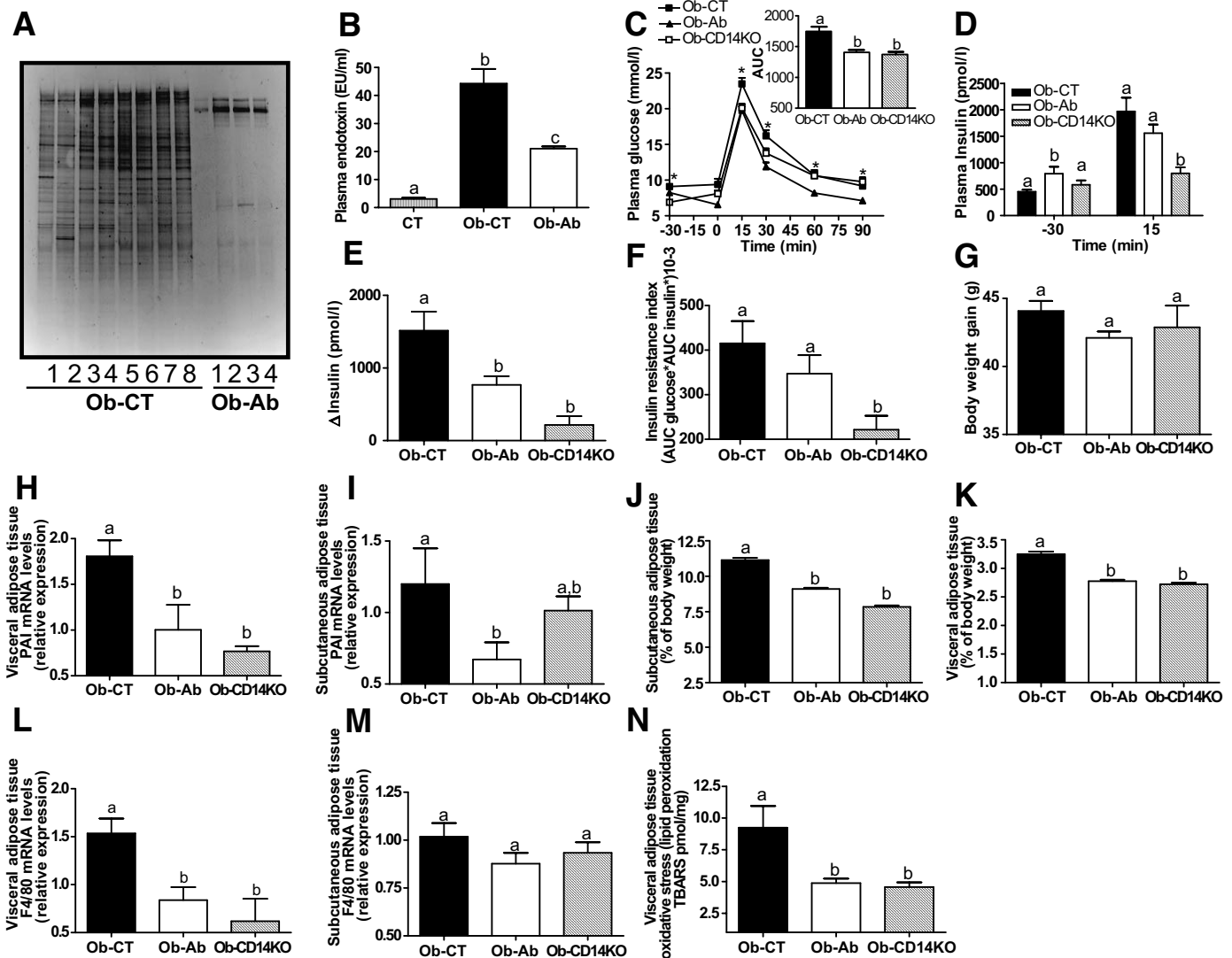


FIG. 7. Antibiotic treatment of *ob/ob* mice reduced endotoxemia. *ob/ob* mice treated with antibiotic and *ob/ob CD14^{-/-}* mice exhibited lower mRNA concentration of adipose tissue inflammatory markers and improved metabolic parameters. **A:** DGGE profiles generated from the cecal microbiota in *ob/ob* mice (Ob) or *ob/ob* mice treated with antibiotic (Ob-Ab) for 4 weeks. Each number and profile correspond to a different animal. **B:** Plasma endotoxin (LPS) concentration (EU/ml). **C:** Plasma glucose (mmol/l) after an oral glucose load (1 g/kg) in *ob/ob* mice (Ob), *ob/ob* mice treated with antibiotics (Ob-Ab) for 4 weeks, or *ob/ob CD14^{-/-}* mice. The inset represents the area under curve (AUC) of the same groups. **D:** Plasma insulin concentration (pmol/l) 30 min before (–30) and 15 min after (15) oral glucose administration of the same groups. **E:** Glucose-induced insulin secretion after oral glucose administration. **F:** Insulin resistance index. **G:** Body weight gain. **H:** Subcutaneous adipose tissue weight (percent body weight). **I:** Visceral adipose tissue weight (percent body weight). **J:** Subcutaneous adipose tissue PAI-1 and F4/80 mRNA concentrations. **K:** Subcutaneous adipose tissue PAI-1 and F4/80 mRNA concentrations in *ob/ob* mice (Ob), *ob/ob* mice treated with antibiotics (Ob-Ab) for 4 weeks, or *ob/ob CD14^{-/-}* mice. **L:** Visceral adipose tissue PAI-1 and F4/80 mRNA concentrations. **M:** Visceral adipose tissue PAI-1 and F4/80 mRNA concentrations in *ob/ob* mice (Ob), *ob/ob* mice treated with antibiotics (Ob-Ab) for 4 weeks, or *ob/ob CD14^{-/-}* mice. **N:** Visceral adipose tissue oxidative stress levels (lipid peroxides concentrations) in the same groups. Data are means ± SE. Data with different superscript letters are significantly different ($P < 0.05$) according to the post hoc ANOVA statistical analysis.

microbiota (4,6). Evidently, the intestinal epithelium acts as a continuous barrier to avoid LPS translocation, but some endogenous or exogenous factors may alter this function. Among the factors promoting a leaky gut and increasing plasma LPS levels, alcohol consumption (29–33), immobilization stress (33,34), and radiation (35) have been put forward. Most importantly, in most of these studies, antibiotic treatments were also administered and resulted in reduced plasma and cecal LPS levels. In addition to these factors, we further showed that reduced endotoxemia was due to a change in the microflora profile. High-fat feeding decreased the number of bifidobacteria (4,6). This group of bacteria has been shown to reduce intestinal LPS levels in mice and to improve the mucosal barrier function (36–38). Furthermore, we have shown

that prebiotics increased the number of bifidobacteria and reduced the impact of high-fat diet-induced metabolic disorders (6). Interestingly, bifidobacteria do not degrade intestinal mucous glycoproteins like other pathogenic bacteria do. This effect promotes a healthier microvillus environment by preventing permeability and bacterial translocation (39,40). In the present study, we further provide evidence that the mechanisms involved in the development of metabolic endotoxemia and the corresponding metabolic disorders in response to high-fat feeding are associated with an increased intestinal permeability. The modulation of gut bacteria after high-fat diet strongly increased intestinal permeability by reducing the expression of genes coding for tight junction proteins ZO-1 and occludin. Moreover, our data demonstrate that gut bacteria are clearly

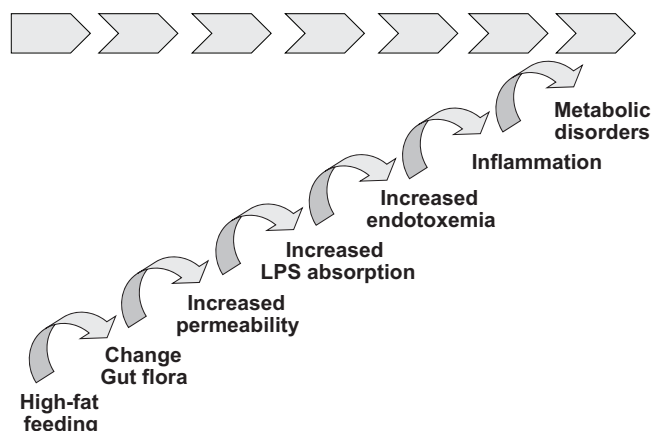


FIG. 8. Hypothesis for bacteria-induced metabolic disease. On excessive high-fat feeding, intestinal microflora changes. This is associated with an increased intestinal permeability. Consequently, endotoxemia increases and triggers inflammation and metabolic disorders.

involved in the present mechanism because antibiotic-treated mice exhibited normal intestinal integrity, although the mice were still eating a high-fat diet. We therefore, suggest that high-fat feeding changes gut microflora, which then increase intestinal LPS permeability (Fig. 1C). It is noteworthy that the antibiotic treatment reduced the intestinal content in LPS, which could contribute as well to the reduced metabolic endotoxemia. We report here that changes in feeding habits or the antibiotic treatment profoundly affect the fecal content in energy. The lipid content was dramatically increased in mice treated with antibiotics, suggesting that intestinal flora contributes to energy harvesting or absorption. This observation is also supported by data from literature (7–12). Together, these data emphasize the role of gut microbiota in the development of high-fat diet-induced metabolic disorders.

These results demonstrate that the gut bacteria determines the threshold at which metabolic endotoxemia occurs during high-fat diet feeding. However, the role of gut microbiota on the development of metabolic endotoxemia-induced inflammation and metabolic disorders is poorly defined. Therefore, we characterized several inflammatory markers and found that the increase in PAI-1, IL-1, and TNF- α mRNA concentrations after high-fat feeding was completely abolished by the antibiotic treatment. This mechanism does not depend on the amount of fat ingested because it was even increased by the antibiotic treatment. Oxidative stress is frequently associated with inflammation and metabolic dysfunction in adipose depots (20–22). We similarly found that the antibiotic treatment totally normalized lipid peroxidation in the visceral adipose depots and normalized the inflammatory/oxidative stress factor STAMP2 (21) and NADPHox mRNA concentration in the visceral and subcutaneous adipose depots. Furthermore, we found that antibiotic-treated mice exhibited normal F4/80 and MCP-1 mRNA concentrations in the visceral adipose depot. Our result are in agreement with data from the literature, because we and others have previously shown that high-fat feeding is associated with adipose tissue macrophage infiltration (F4/80-positive cells) and chemokine MCP-1 (4,41,42). Moreover, our multiple correlation analyses strongly suggest that inflammation, macrophage infiltration, and oxidative stress

markers are induced by LPS-dependent mechanisms and controlled by the antibiotic treatment. We here also further demonstrated that the modulation of gut microbiota improved high-fat diet-induced glucose intolerance, body weight gain, and fat mass development. These results are in line with our and other previous data showing that in the absence of metabolic endotoxemia or LPS receptor, dietary lipids are not sufficient to induce metabolic disorders (4,6,25,28).

To assess the contribution of gut microbiota to the development of metabolic endotoxemia and inflammation regardless of the high-fat feeding, we focused on *ob/ob* mice. These animals are characterized by different gut microbiota (8,12), higher inflammatory tone, and endotoxemia when compared with wild-type mice (23). Antibiotic treatment dramatically changed the *ob/ob* mice gut microbiota; reduced *Lactobacillus* spp., *Bifidobacterium* spp., and *Bacteroides-Prevotella* spp.; and lowered metabolic endotoxemia. Furthermore, these parameters were associated with a significantly lower inflammatory tone in *ob/ob* antibiotic-treated mice. To demonstrate that the LPS receptor is involved in the regulation of inflammation and metabolic disorders in response to changes of gut microbiota, we therefore generated *ob/ob* mice lacking the LPS receptor CD14 (*ob/ob CD14^{-/-}*). Inflammation and macrophage infiltration markers were reduced in the visceral adipose depots and to a lower extent in the subcutaneous adipose depots of *ob/ob CD14^{-/-}* mice. The latter set of data demonstrates that metabolic endotoxemia measured in *ob/ob* mice is, at least in part, involved in the inflammatory phenotype. In *ob/ob* mice, the lowering of metabolic endotoxemia, by means of the antibiotic treatment, and of LPS action in the *ob/ob CD14^{-/-}* mice are associated with a significantly increased glucose tolerance and reduced visceral and subcutaneous adipose depots weight. Interestingly, we also found that *ob/ob* mice treated for 4 weeks with an endotoxin inhibitor (43) administered via osmotic mini-pumps improved glucose tolerance and lowered adipose tissue fat mass (Supplemental Fig. 2). This pattern is similar to that observed in antibiotic-treated mice. This confirms that the gut microflora and the consequent increased bacteria-derived factor LPS exert a key role in the development of adipose depots and inflammation in *ob/ob* mice. Altogether, these data demonstrate that changes in gut microbiota and metabolic endotoxemia play a role in the *ob/ob* phenotype.

In the quest for non-gut-dependent sources of endotoxemia, periodontitis could also be linked to the development of metabolic disorders (44). Several studies reported that the treatment of periodontitis with antibiotics was associated with improved metabolic parameters (45). Nevertheless, the impact of such antibiotic treatment on gut microbiota has not been investigated but could play a part in the improved metabolic phenotype.

In summary, first, we have demonstrated that in high-fat diet-fed mice, the modulation of gut microbiota is associated with an increased intestinal permeability that precedes the development of metabolic endotoxemia, inflammation, and associated disorders (Fig. 8). Second, we found that in *ob/ob* mice, gut microbiota determines the concentration of plasma LPS and is a mechanism involved in metabolic disorders. Altogether, we demonstrate that gut microbiota sets the threshold for metabolic endotoxemia.

ACKNOWLEDGMENTS

P.D.C. is a postdoctoral researcher from the Fonds de la Recherche Scientifique (Belgium) and recipient of subsidies from Fonds speciaux de recherche, Université Catholique de Louvain (UCL) (Belgium). N.M.D. is the recipient of subsidies from Fonds speciaux de recherche, UCL (Belgium). R.B. is the recipient of subsidies from the Nutritia Foundation, the Association Française Etude et de Recherche sur les obésités, l'Agence National de la Recherche (Programme ANR-05-PNRA-004 Nutrisens, PNRA-005.13 MitHyCal, PNRA-30032006-01-03 Metaprofile), the Institut National de la Santé et de la Recherche Médicale, the Université Paul Sabatier, and the Club d'étude du système nerveux autonome.

We thank Dr. C. Feyt and Dr. G. Muccioli for helpful criticisms and F. De Backer, A. Stroobants, A. Colom, and C. Chabo for excellent technical assistance.

REFERENCES

- Kahn SE, Hull RL, Utzschneider KM: Mechanisms linking obesity to insulin resistance and type 2 diabetes. *Nature* 444:840–846, 2006
- Hotamisligil GS: Inflammation and metabolic disorders. *Nature* 444:860–867, 2006
- Wellen KE, Hotamisligil GS: Inflammation, stress, and diabetes. *J Clin Invest* 115:1111–1119, 2005
- Cani PD, Amar J, Iglesias MA, Poggi M, Knauf C, Bastelica D, Neyrinck AM, Fava F, Tuohy KM, Chabo C, Waget A, Delmee E, Cousin B, Sulpice T, Chamontin B, Ferrieres J, Tanti JF, Gibson GR, Casteilla L, Delzenne NM, Alessi MC, Burcelin R: Metabolic endotoxaemia initiates obesity and insulin resistance. *Diabetes* 56:1761–1772, 2007
- Cani PD, Knauf C, Iglesias MA, Drucker DJ, Delzenne NM, Burcelin R: Improvement of glucose tolerance and hepatic insulin sensitivity by oligofructose requires a functional glucagon-like peptide 1 receptor. *Diabetes* 55:1484–1490, 2006
- Cani PD, Neyrinck AM, Fava F, Knauf C, Burcelin RG, Tuohy KM, Gibson GR, Delzenne NM: Selective increases of bifidobacteria in gut microflora improve high-fat-diet-induced diabetes in mice through a mechanism associated with endotoxaemia. *Diabetologia* 50:2374–2383, 2007
- Ley RE, Turnbaugh PJ, Klein S, Gordon JI: Microbial ecology: human gut microbes associated with obesity. *Nature* 444:1022–1023, 2006
- Turnbaugh PJ, Ley RE, Mahowald MA, Magrini V, Mardis ER, Gordon JI: An obesity-associated gut microbiome with increased capacity for energy harvest. *Nature* 444:1027–1031, 2006
- Backhed F, Manchester JK, Semenkovich CF, Gordon JI: Mechanisms underlying the resistance to diet-induced obesity in germ-free mice. *Proc Natl Acad Sci U S A* 104:979–984, 2007
- Backhed F, Ley RE, Sonnenburg JL, Peterson DA, Gordon JI: Host-bacterial mutualism in the human intestine. *Science* 307:1915–1920, 2005
- Backhed F, Ding H, Wang T, Hooper LV, Koh GY, Nagy A, Semenkovich CF, Gordon JI: The gut microbiota as an environmental factor that regulates fat storage. *Proc Natl Acad Sci U S A* 101:15718–15723, 2004
- Ley RE, Backhed F, Turnbaugh P, Lozupone CA, Knight RD, Gordon JI: Obesity alters gut microbial ecology. *Proc Natl Acad Sci U S A* 102:11070–11075, 2005
- Ferrier L, Berard F, Debrauwer L, Chabo C, Langella P, Bueno L, Fioramonti J: Impairment of the intestinal barrier by ethanol involves enteric microflora and mast cell activation in rodents. *Am J Pathol* 168:1148–1154, 2006
- Tannock GW, Munro K, Harmsen HJ, Welling GW, Smart J, Gopal PK: Analysis of the fecal microflora of human subjects consuming a probiotic product containing *Lactobacillus rhamnosus* DR20. *Appl Environ Microbiol* 66:2578–2588, 2000
- Futatsugi A, Nakamura T, Yamada MK, Ebisui E, Nakamura K, Uchida K, Kitaguchi T, Takahashi-Iwanaga H, Noda T, Aruga J, Mikoshiba K: IP₃ receptor types 2 and 3 mediate exocrine secretion underlying energy metabolism. *Science* 309:2232–2234, 2005
- Jeejeebhoy KN, Ahmad S, Kozak G: Determination of fecal fats containing both medium and long chain triglycerides and fatty acids. *Clin Biochem* 3:157–163, 1970
- Goossens D, Jonkers D, Russel M, Stobberingh E, van den BA, Stockbrugger R: The effect of *Lactobacillus plantarum* 299v on the bacterial composition and metabolic activity in faeces of healthy volunteers: a placebo-controlled study on the onset and duration of effects. *Aliment Pharmacol Ther* 18:495–505, 2003
- Goris H, de Boer F, van der Waaij D: Oral administration of antibiotics and intestinal flora associated endotoxin in mice. *Scand J Infect Dis* 18:55–63, 1986
- Wang Q, Fang CH, Hasselgren PO: Intestinal permeability is reduced and IL-10 levels are increased in septic IL-6 knockout mice. *Am J Physiol Regul Integr Comp Physiol* 281:R1013–R1023, 2001
- Furukawa S, Fujita T, Shimabukuro M, Iwaki M, Yamada Y, Nakajima Y, Nakayama O, Makishima M, Matsuda M, Shimomura I: Increased oxidative stress in obesity and its impact on metabolic syndrome. *J Clin Invest* 114:1752–1761, 2004
- Wellen KE, Fucho R, Gregor MF, Furuhashi M, Morgan C, Lindstad T, Vaillancourt E, Gorgun CZ, Saatcioglu F, Hotamisligil GS: Coordinated regulation of nutrient and inflammatory responses by STAMP2 is essential for metabolic homeostasis. *Cell* 129:537–548, 2007
- Houstis N, Rosen ED, Lander ES: Reactive oxygen species have a causal role in multiple forms of insulin resistance. *Nature* 440:944–948, 2006
- Brun P, Castagliuolo I, Leo VD, Buda A, Pinzani M, Palu G, Martines D: Increased intestinal permeability in obese mice: new evidence in the pathogenesis of nonalcoholic steatohepatitis. *Am J Physiol Gastrointest Liver Physiol* 292:G518–G525, 2007
- Poggi M, Bastelica D, Gual P, Iglesias MA, Gremeaux T, Knauf C, Peiretti F, Verdier M, Juhán-Vague I, Tanti JF, Burcelin R, Alessi MC: C3H/HeJ mice carrying a toll-like receptor 4 mutation are protected against the development of insulin resistance in white adipose tissue in response to a high-fat diet. *Diabetologia* 50:1267–1276, 2007
- Shi H, Kokoeva MV, Inouye K, Tzameli I, Yin H, Flier JS: TLR4 links innate immunity and fatty acid-induced insulin resistance. *J Clin Invest* 116:3015–3025, 2006
- Song MJ, Kim KH, Yoon JM, Kim JB: Activation of Toll-like receptor 4 is associated with insulin resistance in adipocytes. *Biochem Biophys Res Commun* 346:739–745, 2006
- Suganami T, Mieda T, Itoh M, Shimoda Y, Kamei Y, Ogawa Y: Attenuation of obesity-induced adipose tissue inflammation in C3H/HeJ mice carrying a Toll-like receptor 4 mutation. *Biochem Biophys Res Commun* 354:45–49, 2007
- Tsukumo DM, Carvalho-Filho MA, Carvalheira JB, Prada PO, Hirabara SM, Schenka AA, Araujo EP, Vassallo J, Curi R, Velloso LA, Saad MJ: Loss-of-function mutation in Toll-like receptor 4 prevents diet-induced obesity and insulin resistance. *Diabetes* 56:1986–1998, 2007
- Nishida J, Ekataksin W, McDonnell D, Urbaschek R, Urbaschek B, McCuskey RS: Ethanol exacerbates hepatic microvascular dysfunction, endotoxaemia, and lethality in septic mice. *Shock* 1:413–418, 1994
- Adachi Y, Moore LE, Bradford BU, Gao W, Thurman RG: Antibiotics prevent liver injury in rats following long-term exposure to ethanol. *Gastroenterology* 108:218–224, 1995
- Enomoto N, Ikejima K, Yamashina S, Hirose M, Shimizu H, Kitamura T, Takei Y, Sato AN, Thurman RG: Kupffer cell sensitization by alcohol involves increased permeability to gut-derived endotoxin. *Alcohol Clin Exp Res* 25:51S–54S, 2001
- Enomoto N, Ikejima K, Bradford B, Rivera C, Kono H, Brenner DA, Thurman RG: Alcohol causes both tolerance and sensitization of rat Kupffer cells via mechanisms dependent on endotoxin. *Gastroenterology* 115:443–451, 1998
- Rivera CA, Bradford BU, Seabra V, Thurman RG: Role of endotoxin in the hypermetabolic state after acute ethanol exposure. *Am J Physiol* 275:G1252–G1258, 1998
- Rivera CA, Tchamatchi MH, Mendoza L, Smith CW: Endotoxaemia and hepatic injury in a rodent model of hindlimb unloading. *J Appl Physiol* 95:1656–1663, 2003
- Paulos CM, Wrzesinski C, Kaiser A, Hinrichs CS, Chieppa M, Cassard L, Palmer DC, Boni A, Muranski P, Yu Z, Gattinoni L, Antony PA, Rosenberg SA, Restifo NP: Microbial translocation augments the function of adoptively transferred self/tumor-specific CD8 T cells via TLR4 signaling. *J Clin Invest* 117:2197–2204, 2007
- Wang Z, Xiao G, Yao Y, Guo S, Lu K, Sheng Z: The role of bifidobacteria in gut barrier function after thermal injury in rats. *J Trauma* 61:650–657, 2006
- Griffiths EA, Duffy LC, Schanbacher FL, Qiao H, Dryja D, Leavens A, Rossman J, Rich G, Dirienzo D, Ogra PL: In vivo effects of bifidobacteria and lactoferrin on gut endotoxin concentration and mucosal immunity in Balb/c mice. *Dig Dis Sci* 49:579–589, 2004
- Wang ZT, Yao YM, Xiao GX, Sheng ZY: Risk factors of development of gut-derived bacterial translocation in thermally injured rats. *World J Gastroenterol* 10:1619–1624, 2004

39. Caplan MS, Miller-Catchpole R, Kaup S, Russell T, Lickerman M, Am M, Xiao Y, Thomson R Jr: Bifidobacterial supplementation reduces the incidence of necrotizing enterocolitis in a neonatal rat model. *Gastroenterology* 117:577–583, 1999
40. Ruseler-van Embden JG, van Lieshout LM, Gosselink MJ, Marteau P: Inability of *Lactobacillus casei* strain GG, *L. acidophilus*, and *Bifidobacterium bifidum* to degrade intestinal mucus glycoproteins. *Scand J Gastroenterol* 30:675–680, 1995
41. Weisberg SP, McCann D, Desai M, Rosenbaum M, Leibel RL, Ferrante AW Jr: Obesity is associated with macrophage accumulation in adipose tissue. *J Clin Invest* 112:1796–1808, 2003
42. Kanda H, Tateya S, Tamori Y, Kotani K, Hiasa K, Kitazawa R, Kitazawa S, Miyachi H, Maeda S, Egashira K, Kasuga M: MCP-1 contributes to macrophage infiltration into adipose tissue, insulin resistance, and hepatic steatosis in obesity. *J Clin Invest* 116:1494–1505, 2006
43. Rustici A, Velucchi M, Faggioni R, Sironi M, Ghezzi P, Quataert S, Green B, Porro M: Molecular mapping and detoxification of the lipid A binding site by synthetic peptides. *Science* 259:361–365, 1993
44. Saito T, Hayashida H, Furugen R: Comment on: Cani et al: (2007) Metabolic endotoxemia initiates obesity and insulin resistance. *Diabetes* 56:1761–1772. *Diabetes* 56:e20, 2007
45. Janket SJ, Wightman A, Baird AE, Van Dyke TE, Jones JA: Does periodontal treatment improve glycemic control in diabetic patients? A meta-analysis of intervention studies. *J Dent Res* 84:1154–1159, 2005